Journal of Biomedical Optics 9(2), 367–371 (March/April 2004)

Pump-probe detection of laser-induced microbubble formation in retinal pigment epithelium cells

Jan Roegener
Wellman Laboratories of Photomedicine
Massachusetts General Hospital
Harvard Medical School
Boston, Massachusetts 02114
and
University of Bielefeld
Applied Laserphysics D3
Universitaetsstrasse 25
33615 Bielefeld, Germany

Ralf Brinkmann
Medical Laser Center Luebeck
Luebeck, Germany

Charles P. Lin
Wellman Laboratories of Photomedicine
Massachusetts General Hospital
Harvard Medical School
Boston, Massachusetts 02114

Abstract. Microsecond laser pulses are currently being investigated in a new ophthalmic procedure for treatment of disorders associated with the retinal pigment epithelium (RPE). The precise mechanism for microsecond laser-induced RPE damage, however, has not been determined. We have previously shown that short pulse laser irradiation in the nanosecond to picosecond time domain causes transient microbubble formation around melanin granules in pigmented cells. Nanosecond time-resolved microscopy was previously used to visualize the intracellular cavitation dynamics. However, this technique is difficult to use with microsecond laser exposures, especially when multiple laser pulses are applied in a rapid sequence as in the clinical setting. Here we describe a simple pump-probe method for detecting transient light scattering signal from individual RPE cells when they are irradiated with nanosecond and microsecond laser pulses. For single 12 ns pulses the threshold for bubble detection was the same as the ED_{50} threshold for cell death. For 6 μs pulse duration the threshold for bubble detection was about 10% higher than the threshold for cell death. With repetitive pulse trains at 500 Hz the ED_{50} decreased about 25% for 10 and 100 pulses. Cells die when a single bubble was detected in a multiple pulse sequence. © *2004 Society of Photo-Optical Instrumentation Engineers.* [DOI: 10.1117/1.1646413]

Keywords: RPE; retinal pigment epithelium; melanosome; pump-probe; cavitation; microbubble.

Paper 03031 received Mar. 19, 2003; revised manuscript received Jul. 11, 2003; accepted for publication Jul. 15, 2003.

1 Introduction

Progress in understanding the mechanism for laser interaction with retinal tissue is driven both by advances in ophthalmic laser therapy and by the need to establish mechanistic underpinning for laser eye safety standards.[1,2] The best understood process for retinal damage involves millisecond and longer laser exposures, where energy deposition into the retinal pigment epithelium (RPE) (the primary absorber) and heat diffusion from this layer to the surrounding tissue result in the thermal coagulation of the retina.[1] On the other hand, increasing evidence points to the existence of a photomechanical damage mechanism when the pulse duration is shorter than $\sim$1 μs.[3–8] As the rate of energy deposition exceeds the rate of thermal relaxation, the energy becomes confined to the absorbing structures—the melanin granules—within the RPE layer. These pigment microparticles form intracellular hot spots and initiate microscopic cavitation bubbles that expand and collapse on the timescale of 0.1–1 μs.[3–5] The mechanical actions associated with microbubble expansion and implosion imparts damage to cells.[4,5,8,9] Previous studies have used a fast time-resolved imaging technique to visualize the transient microbubbles.[3–5] In this method, a laser pulse was applied to heat the particles and a second laser pulse, delayed in time relative to the first, was used to illuminate the sample for stroboscopic image capture. The threshold for bubble formation was found to be the same as the threshold for RPE cell damage—approximately 0.05 J/cm^2 for both 10 ns and 30 ps laser pulses at 532 nm.[3–5]

Microsecond pulse duration falls in the range where transition between the thermal and the mechanical damage processes is expected to take place, although exactly where this changeover occurs has not been determined. Here we describe an optical pump-probe method to detect microbubble formation within the RPE. In this method, bubble formation is detected as a transient increase in the probe beam backscattering signal during the lifetime of the bubble. We have chosen this method over the stroboscopic imaging approach for the current studies based on the following reasons. First, in order to capture a sharp ''stop action'' image of the bubble that expands and collapses rapidly, a nanosecond strobe pulse is required. However, it is difficult to predict exactly when to apply the nanosecond strobe pulse during the relatively long microsecond irradiation time. It is possible to miss a bubble because the strobe pulse is not applied at the right instant. This problem is circumvented using the probe beam method, which measures the time evolution of the bubble dynamics at a single location (in our case a single cell is irradiated and probed). Second, we are studying the mechanism for RPE cell damage from both a single and a train of multiple laser pulses.

Address all correspondence to Charles P. Lin, PhD, Wellman Laboratories of Photomedicine, Massachusetts General Hospital, BHX 630, Harvard Medical School, Boston, MA 02114. Tel: 617-724-3957; Fax: 617-724-2075; E-mail: lin@helix.mgh.harvard.edu

1083-3668/2004/$15.00 © 2004 SPIE

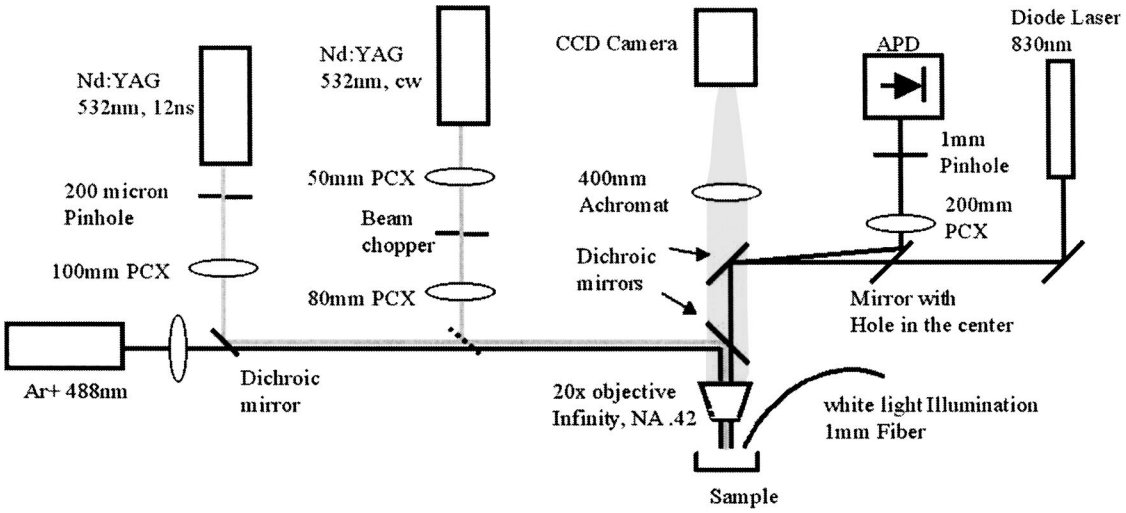

Fig. 1 Pump probe setup to detect microbubble formation in retinal pigment epithelium cells.

When multiple laser pulses are applied at high repetition frequencies, the probe beam method is superior to the stroboscopic imaging approach to determine the probability for bubble formation during the train of multiple laser pulses.

2 Experimental Methods

Porcine eyes of approximately 20 mm diameter were prepared 0–4 h after enucleation. After dissecting the eyes at the equatorial position, the anterior portion and the vitreous were removed. A sheet of 1 cm^2 was cut out of the posterior region of the eye and the sample was suspended in 0.9% saline solution. After 20 min the retina could be easily peeled off. The sample was flattened at the edges using a plastic ring. The RPE was covered with diluted CalceinAM (Molecular Probes) 1 μg/mL in polybutene sulfone or Dulbecco's modified eagle medium (Gibco). A cover slip was applied on top. After 20 min viable cells accumulated enough fluorescent Calcein to be distinguished from dead cells by fluorescence microscopy. Calcein fluorescence was excited at 488 nm and detected with a 540 nm long pass filter. One fluorescence image was taken before and a second 15–30 min after irradiation. Nonfluorescing cells were classified as dead. For 12 ns experiments the sample temperature was 20 °C. This was done to ensure that the measurement condition was the same as that used in previous stroboscopic imaging experiments. Since the temperature required for bubble formation at the surface of the melanosom has been determined to be about 150 °C,[8] a background temperature of 20 or 35 °C was not expected to make a significant difference in the threshold. On the other hand, for 6 μs pulses the sample was kept at a more physiologic temperature of 35 °C in order not to bias our measurement against a potential thermal contribution to the cell death mechanism. The thresholds were calculated using a PC program for probit analyses[10] after Finney.[11]

2.1 *Setup*

A 20× objective (Mitutoyo, numerical aperature=0.42, 25 mm working distance) was used to image the cells onto a charge coupled device camera [Fig. 1]. The spatial resolution of the setup was approximately 1 μm. A frequency doubled, Nd:yttritium–aluminum–garnet (YAG) laser (Continuum, SEO 1-2-3, λ=532 nm, 6 mm beam) was used for 12 ns irradiation. A 200 μm section from the center of the beam was imaged onto the sample to give a flat top image of 20 μm diameter. The intensity variations at the sample due to hot spots in the beam were below 15%, as determined by imaging a fluorescent target within the area of irradiation after making sure that the fluorescence intensity was linear. A continous wave frequency doubled Nd:YAG laser (Verdi, Coherent, λ=532 nm) was used together with a rotating wheel chopper to produce 6 μs pulses at 500 Hz. The gaussian shaped spot has a full width at half maximum (FWHM) of 16 μm at the sample and the average power was 75 mW. To probe the bubble formation the collimated beam of a diode laser (SF830S-18, Microlaser Systems, 830 nm, 1.5×2 mm beam diameter) was focused onto the RPE cell to produce a spot size of 7×10 μm (FWHM) with a maximum power of 1 mW at the sample. For each experiment, the RPE cells were examined through the microscope and the sample stage was positioned so that only one cell (10–15 μm diameter) was in the center of the irradiation laser spot. The probe beam, which was slightly smaller that a REP cell, was always placed on the cell in the center. The probe beam was switched on for less than 10 μs and switched off (1% power) 2–4 μs after the end of the 532 nm laser pulse. Backscattering of the probe beam was detected in a confocal geometry and also slightly off the optical axis to reduce specular reflection and scattering from the optical system and from tissue layers other than the RPE. The detector used was an avalanche photodiode (Hamamatsu C-5460) with a built-in high speed amplifier with 10 MHz bandwidth.

3 Results

3.1 *Nanosecond Exposures*

For 12 ns pulses four samples from four different eyes were used on which a total of 117 spots were irradiated at different fluences (40 controls with the Nd:YAG beam only, 77 with the Nd:YAG plus probe beam). Each irradiation spot was approximately the size of a single RPE cell. Results are listed in

Table 1 Thresholds for 12 ns irradiation with single pulse. Fluence for ED_{50} cell death. Upper (FUL) and lower (FLL) confidential limits and slope of the fit function are a measure of the thresholds accuracy. Control means the cell death threshold as measured without the probe beam.

		FLL	FUL		
	Fluence (mJ/cm^2)	Fluence (mJ/cm^2)	Fluence (mJ/cm^2)	Slope	No. of cells
Cell death	71	66	75	17	77
Cavitation	71	67	75	16	77
Control	71	66	81	14	40

Table 1. The threshold for cavitation bubble detection was the same as the threshold for RPE cell death measured by Calcein fluorescence.

An example of the backscattered probe beam signal at 90 mJ/cm^2 (1.27× threshold) is shown in Fig. 2. The diode laser was switched on at 0.2 μs and switched off at 3.4 μs to minimize sample heating. The pedestal between 0.2 and 3.4 μs is due to backscattering from the RPE tissue. The Nd:YAG laser was fired at 1.2 μs, which caused a transient increase in the backscattering of the probe beam from a single RPE cell. The bubble lifetime was about 500 ns. Both the transient signal and the lifetime increase with increasing radiant exposure, rising up to 2% of the probe beam intensity at several times threshold, which is the maximum expected for a planar air/water interface.

Close to threshold the signals were more difficult to discern. In some events the reflected intensity showed a small increase at the time of irradiation and remained constant for the duration of the probe pulse (several microseconds). Events were classified as positive if the signal increase was greater than 5% of the background during the first 500 ns after the irradiation. Out of the total 77 cells, there were seven false negative and six false positive events within 20% of the ED_{50} threshold, but on average the threshold for bubble detection was the same as the threshold for cell killing (Table 1). At 20% above threshold no cell survived and all cells showed true positive bubble signals.

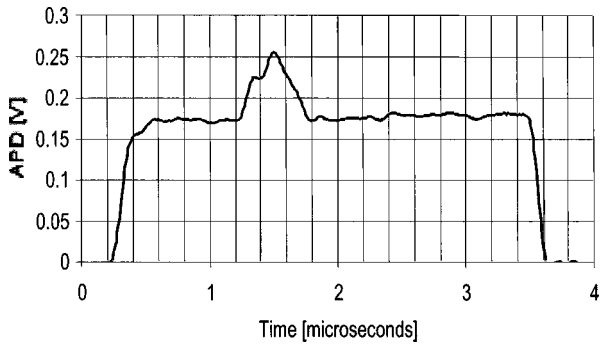

Fig. 2 Signal of backscattered intensity of the probe beam from a 12 ns laser pulse (90 mJ/cm^2). The laser pulse was switched on at 1.2 μs.

Table 2 Thresholds for 6 μs single pulses and pulse trains at 500 Hz. Control refers to cell death threshold for 100 pulses with no probe beam.

			FLL	FUL		
	No. of pulses	Fluence (mJ/cm^2)	Fluence (mJ/cm^2)	Fluence (mJ/cm^2)	Slope	No of cells
Cell death	1	412	386	436	14	105
Cavitation	1	456	425	484	16	105
Cell death	10	306	264	355	12	33
Cavitation	10	381	320	445	11	33
Cell death	100	322	281	359	8	70
Cavitation	100	374	335	413	9	70
Control	100	286	246	338	14	30

3.2 *Microsecond Exposures*

For 6 μs irradiation, four samples from four different eyes were used. A total of 241 cells were irradiated. For each sample, 1, 10, and 100 exposures were applied (at different spots). For single pulses the threshold for bubble detection was 11% higher than the threshold for cell killing. For 10 and 100 pulses the thresholds for bubble detection were 25% and 16% higher, respectively (Table 2). All thresholds decreased with increasing number of pulses. An example of the oscilloscope trace is shown in Fig. 3. At threshold, both the signal amplitude and the bubble lifetime for microsecond laser-induced bubbles were significantly greater than for nanosecond laser-induced bubbles. The lifetime was almost always longer than a microsecond (with only one exception out of ~100 measurements). Cavitation always started before the end of the Nd:YAG laser pulse.

For multiple pulse exposures near threshold, a bubble was often detected in only one or a few pulses (at random) out of the whole sequence (Fig. 4). Whenever, a bubble was detected, even if one occurred only once in the pulse train, the cell was killed. Above threshold, cavitation appeared during each pulse. At threshold, cavitation appeared at arbitrary

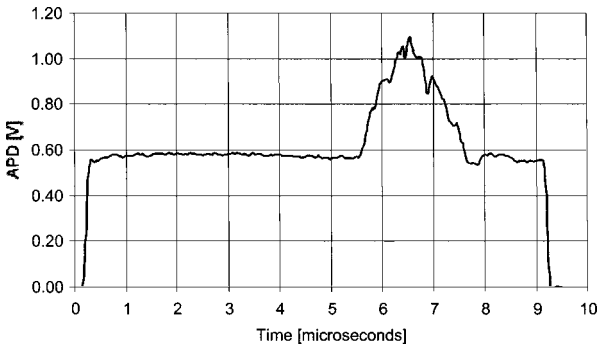

Fig. 3 Signal of the backscatterted intensity of the probe beam from a 6 μs laser pulse (350 mJ/cm^2). The probe beam was switched on at the same time as the irradiation pulse and lasted for 10 μs.

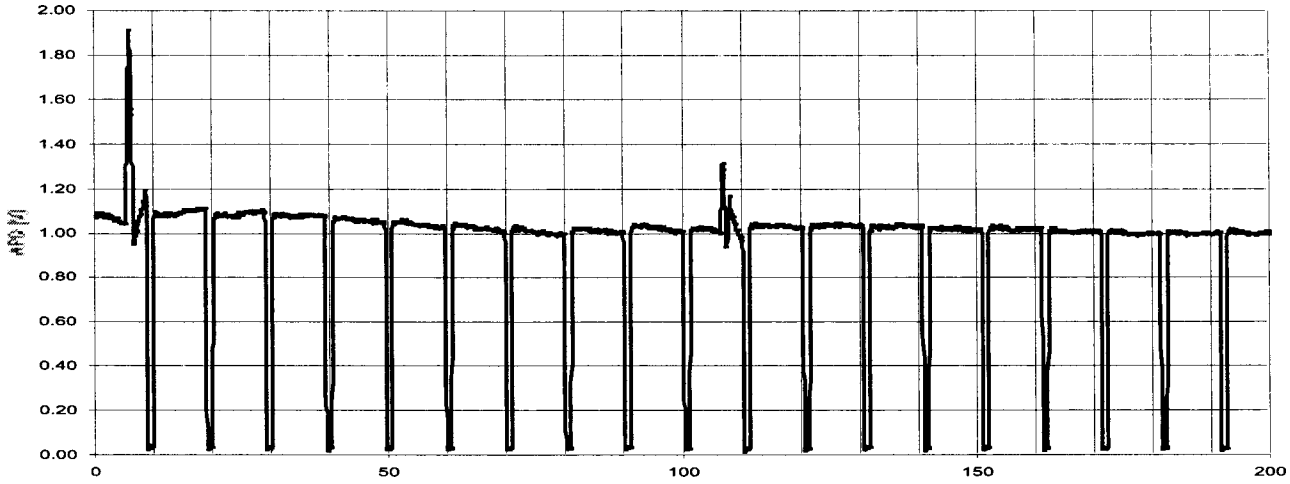

Fig. 4 Signal of the backscatterted intensity of the probe beam from repetitive 6 μs laser pulses (425 mJ/cm^2). Only the first 15 pulses out of a train of 100 pulses are shown in the graph. The probe beam is switched on for 10 μs during and after irradiation. The 2 ms interpulse periods are not shown. Cavitation occurs on pulse 1 and 11.

pulses (Fig. 4), sometimes followed by cavitation within the next pulses, sometimes only at one pulse within the series. The ED_{50} for 100 pulses with probe beam is close to the control (without probe beam).

4 Discussion

For 12 ns pulses the threshold for cell death is the same as for bubble detection using the probe beam method. This is in agreement with Kelly et al. who showed that cell death coincided with intracellular bubble formation detected by the stroboscopic imaging method.[3–5] Although the thresholds were the same (on average), some false positive and some false negative events were observed (six false positive and seven false negative events were detected out of 77 cells within 20% of the ED_{50} threshold). A false positive event means a bubble was detected but the cell survived; a false negative event means bubble was not detected but the cell lost viability. Previous studies have shown, using cultured endothelial cells (EC) containing ingested pigment particles, that that it is possible (but rare) to create small bubbles in the EC without killing the cells.[9] For heavily pigmented cells such as the RPE, which contain numerous pigment granules in each cell, it is expected that irradiation of the particles will produce many bubbles simultaneously within each cell. These bubbles can coalesce to form larger bubbles and most likely cause cell death. Near threshold, however, it is possible that very small bubbles are formed around just 1 or a few melanin granules, giving rise to a bubble signal without killing cells. However, these false positive events were unexpected and the origins of these signals need to be investigated further. False negative signals, on the other hand, could mean either (a) some cells die without cavitation, or (b) cell cavitated but a bubble was not detected. We favor the latter interpretation because the size of the bubble can be much smaller than the size of the RPE cell (the lifetime of the smallest bubble detected was about 200 ns, corresponding to a bubble diameter of about 2 μm). It is possible that bubbles occurring on the edges of the cell were not detected because the probe beam size (FWHM 7 μm$\times$10 μm elliptical) was slightly smaller than the RPE cell (10–15 μm) and also smaller than the excitation spot size (20 μm). The probe beam could be expanded to cover a larger area, but then one has to compromise the sensitivity at the center of the cell (for the same probe laser power).

Occasionally near threshold, the probe beam signal showed a small increase at the time of the laser pulse and remained constant for the duration of the probe pulse (several microseconds). Most likely this signal is due to change in backscattering of the RPE cell as a result of spatial rearrangement or alteration of the melanosomes following the laser pulse. Since these events happened rarely and very close to the threshold with no detectable bubbles, formation of long-lasting bubbles is not likely to be the origin of the signal. For a cavitation bubble to give rise to stable gas bubbles after its collapse, the initial cavity has to be large enough (hundreds of micrometers), with a lifetime long enough (at least tens of microseconds) to allow the dissolved gas to escape into the cavity by ''rectified diffusion.'' The cavitation produced in the RPE cells in our experiments are much too small to produce such stable bubbles (at least none that are visible under the microscope).

With 6 μs pulse duration, which is longer than the thermal relaxation time of a 1 μm melanosome ($\sim$1 μs), there is significant heat diffusion away from the particles during the laser pulse. Consequently the thresholds for cell death (412 mJ/cm^2) and for bubble detection (456 mJ/cm^2) are both higher than for 12 ns pulses. However, this increase in threshold is not as dramatic as the values predicted for bubble formation around a single, isolated melanosome.[7,8] Mutual heating among the closely spaced melanosome particles within the RPE cell can be a significant cause for the temperature increase during the microsecond laser pulses, leading to higher temperatures than an isolated melanosome would reach.[8] Mutual heating is insignificant for 12 ns pulses because there is much less heat diffusion outside the particles.

In general, the threshold bubble signals from 6 μs laser exposures were stronger and had longer lifetimes ($>$1 μs) than the threshold bubble signals from 12 ns laser pulses. A lifetime of 1 μs corresponds to a spherical bubble diameter of

~10 μm. Larger bubbles are expected for microsecond laser pulses because the threshold radiant exposure is higher (a larger volume of surrounding fluid is heated as a result of heat diffusion away from the particle) than for nanosecond pulses.

The ED_{50} values for cell death were comparable with and without the probe beam; indicating that the probe beam did not significantly affect the temperature of the sample. This was shown for 100 pulses and therefore should be true for 1 or 10 pulses. The radiant exposure (~14 mJ/cm^2) produced by probe beam (1 mW, 10 μs long pulse in a 7 μm×10 μm spot) was more than a factor of 20 below the threshold for cell death. In addition, the melanosome absorption at the wavelength of the probe beam (830 nm) was lower than the absorption at 532 nm. Consequently, the probe beam by itself was not expected to have a significant heating effect on the RPE.

The difference between the ED_{50} for cell death and for bubble detection can mean the existence of a damage mechanism that does not involve bubble formation. However, this difference is small (11%) and bubble formation is not ruled out as the mechanism for microsecond laser-induced RPE cell death. Further improvement in bubble detection sensitivity will be necessary to resolve this issue. It is unlikely that strong shock waves are produced without bubble formation because the pulse duration is much longer than the stress confinement time in our experiments. The stress confinement time, or the time for an acoustic wave to travel across the particle, is less than 1 ns for a 1 μm particle.

The threshold declines with multiple pulse exposures. Previous studies have found an empirical relationship between damage threshold and the number of pulses, N, that generally follows the $N^{-1/4}$ power law for thermal damage processes. However, if the damage mechanism is not thermal but is mediated by bubble formation, then it is still possible for the threshold to decline with the number of pulses but not with the $N^{-1/4}$ dependence. An important finding in this study is that a single cavitation event during a long train of pulses is sufficient to kill the cell. Hence, with increasing number of pulses the probability increases for bubble formation in one of the pulses. This is the likely reason for the threshold reduction.

The probe beam technique does not actually image the bubbles. It is independent of the time point at which the bubble arises and can be applied for high repetition multiple pulse exposures. Also this technique can be applied *in vivo* and should be more reliable than getting images of the bubbles *in vivo*. This probe beam technique can become a feedback system for clinical selective RPE treatment.[12–14]

Acknowledgments

This work is supported in part by the Air Force Office of Scientific Research Grant No. F49620-96-1-024 and by NIH R01 EY 12970. The authors thank Dr. C. P. Cain for providing the program for probit analyses.

References

1. D. H. Sliney and M. L. Wolbarsht, *Safety with Lasers and Other Optical Sources*, Plenum, New York (1980).
2. D. H. Sliney and J. Marshall, ''Tissue specific damage to the retinal pigment epithelium: mechanisms and therapeutic implications,'' *Lasers Light in Ophthalmol* **5**, 17–28 (1992).
3. C. P. Lin and M. W. Kelly, ''Cavitation and acoustic emission around laser-heated microparticles,'' *Appl. Phys. Lett.* **72**, 2800–2802 (1998).
4. W. W. Kelly and C. P. Lin, ''Microcavitation and cell injury in RPE cells following short-pulsed laser irradiation,'' *Proc. SPIE* **2975**, 174–179 (1997).
5. C. P. Lin, M. W. Kelly, S. A. Sibayan, M. A. Latina, and R. R. Anderson, ''Selective cell killing by microparticle absorption of pulsed laser radiation,'' *IEEE J. Sel. Top. Quantum Electron.* **5**, 963–968 (1999).
6. V. K. Pustovalov, ''Thermal processes under the action of laser radiation pulse on absorbing granules in heterogeneous biotissues,'' *Int. J. Heat Mass Transfer* **36**, 391–399 (1993).
7. B. S. Gerstman, C. R. Thompson, S. L. Jacques, and M. E. Rogers, ''Laser induced bubble formation in the retina,'' *Lasers Surg. Med.* **18**, 10–21 (1996).
8. R. Brinkmann, G. Hüttmann, J. Rögener, J. Roider, R. Birngruber, and C. P. Lin, ''Origin of RPE-cell damage by pulsed laser irradiance in the ns to μs time regime,'' *Lasers Surg. Med.* **27**, 451–464 (2000).
9. D. Leszczynski, C. M. Pitsillides, R. R. Anderson, and C. P. Lin, ''Laser-beam-triggered microcavitation: a novel method for selective cell destruction,'' *Radiat. Res.* **156**, 399–407 (2001).
10. C. P. Cain, G. D. Noojin, and L. Manning, ''A comparison of various probit methods for analyzing yes/no data on a log scale,'' US Air Force Armstrong Laboratory, AL/OE-TR-1996-0102 (1996).
11. D. J. Finney, *Probit Analysis*, 3rd ed., Cambridge University Press, London (1971).
12. J. Roider, N. A. Michaud, T. J. Flotte, and R. Birngruber, ''Response of the retinal pigment epithelium to selective photocoagulation,'' *Arch. Ophthalmol. (Chicago)* **110**, 1786–1792 (1992).
13. J. Roider, F. Hillenkamp, T. J. Flotte, and R. Birngruber, ''Microphotocoagulation: selective effects of repetitive short laser pulses,'' *Proc. Natl. Acad. Sci. U.S.A.* **90**, 8463–8647 (1993).
14. J. Roider, R. Brinkmann, C. Wirbelauer, H. Laqua, and R. Birngruber, ''Retinal sparing by selective retinal pigment epithelial photocoagulation,'' *Arch. Ophthalmol. (Chicago)* **117**, 1028–1034 (1999).